

## CENTRAL SCHEMES FOR BALANCE LAWS OF RELAXATION TYPE\*

SALVATORE FABIO LIOTTA<sup>†</sup>, VITTORIO ROMANO<sup>‡</sup>, AND GIOVANNI RUSSO<sup>§</sup>

**Abstract.** Several models in mathematical physics are described by quasi-linear hyperbolic systems with source term and in several cases the production term can become stiff. Here suitable central numerical schemes for such problems are developed and applications to the Broadwell model and extended thermodynamics are presented.

The numerical methods are a generalization of the Nessyahu–Tadmor scheme to the nonhomogeneous case by including the cell averages of the production terms in the discrete balance equations. A second order scheme uniformly accurate in the relaxation parameter is derived and its properties analyzed. Numerical tests confirm the accuracy and robustness of the scheme.

**Key words.** central schemes, conservation laws, relaxation, stiff systems

**AMS subject classifications.** 65M99, 65L06, 82D05

**PII.** S0036142999363061

**1. Introduction.** In several problems of mathematical physics, hyperbolic systems of balance laws arise. In particular we mention hyperbolic systems with relaxation, such as discrete velocity models in kinetic theory [1], gas with vibrational degrees of freedom [2], hydrodynamical models for semiconductors [3, 4], and radiation hydrodynamics [5].

Lately the development of high order shock-capturing methods for conservation laws has become an interesting area of research (see, for example, [6, 7, 8]). However, most schemes deal almost exclusively with the homogeneous case. The extension to systems with a source term has been studied mainly in the context of upwind methods [9, 10, 11] where a method of line approach, together with splitting techniques, has been used. Most of such schemes are based on the solution to the Riemann problem. There are systems with relaxation for which the analytical expression of the eigenvalues and eigenvectors is not known. Typical examples are given by monatomic gas in extended thermodynamics and some hydrodynamical models for electron transport in semiconductors. For such systems, schemes based on the solution of the Riemann problem are expensive or impractical.

An alternative approach to upwind schemes for the solution of systems of conservation laws is given by central schemes, which have recently attracted great attention, mainly because of their simplicity and robustness. Central schemes, in fact, require neither the (exact or approximate) solution to the Riemann problem nor the knowledge of the characteristic structure of the Jacobian matrix. The first order, building

---

\*Received by the editors October 15, 1999; accepted for publication (in revised form) May 14, 2000; published electronically October 31, 2000. This work was partially supported by MURST, and by CNR project *Modelli matematici per semiconduttori. Progetto speciale: metodi matematici in fluidodinamica e dinamica molecolare*, grant 96.03855.CT01, by *Convenzione Quadro Università di Catania—ST Microelectronics* 1997-99 and by TMR program *Asymptotic methods in kinetic theory*, grant ERBFMRXCT970157.

<http://www.siam.org/journals/sinum/38-4/36306.html>

<sup>†</sup> Dipartimento di Matematica, Università di Catania, viale A. Doria 6, 95125 Catania, Italy (liotta@dipmat.unict.it)

<sup>‡</sup> Dipartimento Interuniversitario di Matematica, Politecnico di Bari, via E. Orabona 4, 70125 Bari, Italy (romano@dipmat.unict.it)

<sup>§</sup> Università dell'Aquila, Via Vetoio, loc. Coppito, 67100 L'Aquila (russo@univaq.it)

block of central schemes is the Lax–Friedrichs scheme. A second order nonoscillatory scheme was introduced by Nessyahu and Tadmor [12] for one dimensional problems. Central schemes in two dimensions have been derived and studied by several authors [13, 14, 15]. Higher order central schemes have also been developed in one dimension [16, 17, 18], and in several dimensions [19, 20].

Most central schemes are based on the use of a staggered grid in space-time. Recently a new approach has been proposed, which combines the central approach with the method of lines [21]. Such a method has been successfully applied to convection-diffusion problems and seems very promising to obtain numerical solutions of systems with (stiff or nonstiff) source term. We remark that other high order shock-capturing schemes have been constructed that are not based on characteristic decomposition of the system (see, for example, [22]). Whether such schemes are called “central” or “upwind” depends more on the derivation than on the actual resulting scheme.

Here we consider the extension of second order central schemes to the nonhomogeneous case. The aim is to provide a general-purpose robust scheme for systems of balance laws, valid in all the regimes, i.e., when the relaxation time ranges from zero to infinity.

Central schemes with source have been considered in [23, 24]. In the first paper, central schemes for systems of conservation laws are extended to systems with nonstiff source, with particular application to the system of shallow water. In the second paper, a numerical scheme is derived for systems with a (possibly stiff) relaxation term. The authors are aware that Strang splitting is not able to guarantee second order accuracy in the stiff case and propose a nonsplitting strategy which reduces to the second order Nessyahu–Tadmor scheme when the relaxation term is omitted. Their scheme can be written as a predictor-corrector scheme, with an implicit treatment of the source. Its structure, however, is different from the schemes that we propose.

In this paper we consider a family of schemes, which extend the Nessyahu–Tadmor scheme [12] to systems with source. This is done by including the source term in the integration over the cells in space-time. Explicit and implicit formulations are considered. In particular, an implicit scheme which is able to treat stiff source term is derived and analyzed. Splitting strategies have been successfully developed in the context of upwind schemes [10, 11]. However, the approach used in [11] cannot be straightforwardly extended to the Nessyahu–Tadmor central scheme (see [25] and [26] for splitting central schemes).

Here only nonsplitting schemes are considered. This work may be considered an extension of previous works on central schemes and on the proper treatment of stiff source in upwind schemes, although the scheme we present for the treatment of the source and the analysis are original.

If an appropriate quadrature formula is employed for the integration of the production terms, then the scheme retains a full second order accuracy both for stiff and nonstiff source. For a splitting strategy used in conjunction with central schemes, the reader is referred to [25]. However, the splitting schemes, although sufficiently robust for the applications, suffer a loss of accuracy in the fluid regime.

The schemes have been tested on the Broadwell model and the equations for a monatomic gas in extended thermodynamics and accurate results have been obtained.

The plan of the paper is the following. In section 2, a sketch of the mathematical models is given. In sections 3 the method of Nessyahu and Tadmor (hereafter NT) for homogeneous hyperbolic systems is recalled. In section 4 the numerical schemes obtained by including the cell average of the production term are presented and their

analysis is performed in the next section. Numerical tests and applications to extended thermodynamics are reported in the last two sections.

**2. The mathematical models.** Here we present some significant physical models represented by hyperbolic systems of balance laws of relaxation type.

We recall that the system of the type

$$(2.1) \quad \partial_t U + \partial_x F(U) = -\frac{1}{\varepsilon} R(U), \quad U \in \mathbf{R}^N,$$

is said to be a *relaxation system* in the sense of Whitham [27] and Liu [28] if there exists a constant  $n \times N$  matrix  $Q$  with rank  $n < N$  such that  $QR(U) = 0 \forall U$ .

This yields  $n$  independent conserved quantities  $v = QU$ . One assumes that each such  $v$  uniquely determines a local equilibrium value  $U = \mathcal{E}(v)$  satisfying  $R(\mathcal{E}(v)) = 0$ . The image of  $\mathcal{E}$  then constitutes the manifold of local equilibria of  $R$ .

Associated with the original system and the matrix  $Q$  are  $n$  conservation laws which are satisfied by every solution of (2.1)

$$\partial_t QU + \partial_x(QF(U)) = 0 \quad \text{with } U = \mathcal{E}(v) .$$

These equations form a closed system (the reduced system or the equilibrium subsystem) for  $v = QU$  if we take the local relaxation approximation

$$U = \mathcal{E}(v).$$

Such a system has the form

$$\frac{\partial v}{\partial t} + \frac{\partial \mathcal{F}}{\partial x} = 0,$$

where  $\mathcal{F}(v) = QF(\mathcal{E}(v))$ .

When  $\varepsilon$  is small compared to the time scale determined by the characteristic speed of the system, we have a stiff relaxation term.

In the following we shall present two models of relaxation type with stiff source: the Broadwell model and the model of extended thermodynamics for monatomic gas. The first one is an example of a semilinear hyperbolic system while the second one is a quasi-linear hyperbolic system.

**2.1. The Broadwell model.** The Broadwell model describes a two dimensional (three dimensional) gas composed of particles with four (six) discrete velocities with binary collision law and spatial variation in only one direction. For the two dimensional gas the evolution equations read [11]

$$(2.2) \quad \partial_t \rho + \partial_x m = 0,$$

$$(2.3) \quad \partial_t m + \partial_x z = 0,$$

$$(2.4) \quad \partial_t z + \partial_x m = \frac{1}{\varepsilon}(\rho^2 + m^2 - 2\rho z),$$

where  $\varepsilon$  is the mean free path. The dynamical variables  $\rho$  and  $m$  are the density and the momentum, respectively, while  $z$  represents the flux of momentum.

The characteristic velocities are constant,

$$\lambda = -1, 0, 1.$$

As  $\varepsilon \rightarrow 0$ ,  $z$  is given by a local Maxwellian distribution

$$(2.5) \quad z = z_E(\rho, m) = \frac{1}{2\rho}(\rho^2 + m^2)$$

and we are in the fluid dynamic limit, satisfying the equations

$$\begin{aligned} \partial_t \rho + \partial_x(\rho u) &= 0, \\ \partial_t(\rho u) + \partial_x\left(\frac{1}{2}(\rho + \rho u^2)\right) &= 0, \end{aligned}$$

with  $u = m/\rho$ .

**2.2. The model of extended thermodynamics for monatomic gas.** The extended thermodynamics [29, 30] describes nonequilibrium phenomena in continuum mechanics by treating the dissipative variables as additional evolution variables. Therefore the balance equations also comprise, in addition to the conservation equations for density, momentum, and energy, further balance equations for the viscous stress tensor and the heat flux.

In the one dimensional case the model is given by the following evolution equations:

$$(2.6) \quad \frac{\partial \rho}{\partial t} + \frac{\partial}{\partial x}(\rho u) = 0,$$

$$(2.7) \quad \frac{\partial}{\partial t}(\rho u) + \frac{\partial}{\partial x}(\rho u^2 + p + \sigma) = 0,$$

$$(2.8) \quad \frac{\partial}{\partial t}\left(\frac{1}{2}\rho u^2 + \frac{3}{2}p\right) + \frac{\partial}{\partial x}\left(\frac{1}{2}\rho u^3 + \frac{5}{2}up + \sigma u + q\right) = 0,$$

$$(2.9) \quad \frac{\partial}{\partial t}\left(\frac{2}{3}\rho u^2 + \sigma\right) + \frac{\partial}{\partial x}\left(\frac{2}{3}\rho u^3 + \frac{4}{3}up + \frac{7}{3}u\sigma + \frac{8}{15}q\right) = -\frac{\rho\sigma}{\varepsilon},$$

$$(2.10) \quad \begin{aligned} \frac{\partial}{\partial t}(\rho u^3 + 5up + 2\sigma u + 2q) + \frac{\partial}{\partial x}\left(\rho u^4 + 5\frac{p^2}{\rho} + 7\frac{\sigma p}{\rho} + \frac{32}{5}qu + u^2(8p + 5\sigma)\right) \\ = -\frac{2\rho}{\varepsilon}\left(\frac{2}{3}q + \sigma u\right), \end{aligned}$$

where  $\rho$  is the density,  $u$  is the velocity,  $p$  is the pressure,  $\sigma$  is the  $xx$ -component of the viscous stress tensor, and  $q$  is the heat flux. In the case of a monatomic gas,  $\varepsilon$  is a constant and  $\rho/\varepsilon$  is the inverse of the relaxation time for  $\sigma$ .

System (2.6)–(2.11) is hyperbolic in a suitable region of the space variable (see [29]).

As in the Broadwell model, when  $\varepsilon$  is small compared to the speed given by the characteristic velocity of the system, the problem becomes stiff. Moreover, as  $\varepsilon \rightarrow 0$ , the local equilibrium subsystem is given by the usual Euler equations for a monatomic gas,

$$(2.11) \quad \frac{\partial \rho}{\partial t} + \frac{\partial}{\partial x}(\rho u) = 0,$$

$$(2.12) \quad \frac{\partial}{\partial t}(\rho u) + \frac{\partial}{\partial x}(\rho u^2 + p) = 0,$$

$$(2.13) \quad \frac{\partial}{\partial t}\left(\frac{1}{2}\rho u^2 + \frac{3}{2}p\right) + \frac{\partial}{\partial x}\left(\frac{1}{2}\rho u^3 + \frac{5}{2}up\right) = 0.$$

We remark that explicit analytical expressions for the eigenvalues and eigenvectors of the system (2.6)–(2.11) are not known. Therefore in order to integrate numerically the system (2.6)–(2.11), a highly desirable property of the numerical scheme is that it does not require the knowledge of the characteristic structure of the evolution equations. In fact, the use of numerical methods based on the characteristic decomposition such as those obtained with the use of the Roe matrix can be computationally too heavy.

**3. The Nessyahu–Tadmor scheme.** Let us consider the initial value problem

$$(3.1) \quad \frac{\partial u}{\partial t} + \frac{\partial f}{\partial x} = g(u),$$

$$(3.2) \quad u(x, 0) = \Phi(x), \quad -\infty < x < \infty$$

with  $u \in \mathbf{R}^m$  and  $f(u) : \mathbf{R}^m \rightarrow \mathbf{R}^m$ .

The NT numerical method for the homogeneous equation, that is, for  $g(u) = 0$ , has the form of a predictor-corrector scheme

$$(3.3) \quad u_j^{n+1/2} = u_j^n - \frac{\lambda}{2} f'_j,$$

$$(3.4) \quad u_{j+1/2}^{n+1} = \frac{1}{2}(u_j^n + u_{j+1}^n) + \frac{1}{8}(u'_j - u'_{j+1}) - \lambda \left( f(u_{j+1}^{n+1/2}) - f(u_j^{n+1/2}) \right),$$

where  $\lambda = \Delta t / \Delta x$ .

The time step  $\Delta t$  must satisfy the stability condition

$$(3.5) \quad \lambda \max_j \rho(A(u(x_j, t))) < \frac{1}{2},$$

where  $\rho$  denotes the spectral radius of the Jacobian matrix  $A = \partial f / \partial u$ . This condition ensures that the generalized Riemann problems with piecewise smooth data at time  $t_n$  do not interact during the time step  $\Delta t$ .

The values of  $u'_j / \Delta x$  and  $f'_j / \Delta x$  are a first order approximation of the space derivatives of the field and of the flux. They can be computed in several ways (see [12]). The simplest choice is

$$(3.6) \quad u'_j = \text{MM}(u_{j+1} - u_j, u_j - u_{j-1}),$$

where  $\text{MM}(x, y)$  is the min mod function, defined by

$$\text{MM}(x, y) = \begin{cases} \text{sgn}(x) \cdot \min(|x|, |y|) & \text{if } \text{sgn}(x) = \text{sgn}(y), \\ 0 & \text{otherwise.} \end{cases}$$

We shall adopt the UNO-like derivative [31]

$$D_{j+\frac{1}{2}} u = \text{MM}(u_{j+2} - 2u_{j+1} + u_j, u_{j+1} - 2u_j + u_{j-1}),$$

$$u'_j = \text{MM}(u_{j+1} - u_j - \frac{1}{2} D_{j+\frac{1}{2}} u, u_j - u_{j-1} + \frac{1}{2} D_{j-\frac{1}{2}} u)$$

which we find gives the best results among the limiters proposed in [12].

Now we show how to generalize the NT scheme to the nonhomogeneous case, that is, when  $g(u) \neq 0$ . For a strategy based on a splitting schemes the reader is referred to [25].

In developing the numerical schemes we keep in mind the following guidelines:

- truncation error analysis is used to obtain second order accuracy in the rarefied regime ( $\varepsilon=O(1)$ );
- the collision step is well posed  $\forall\varepsilon$  and its solution relaxes to a local Maxwellian as  $\varepsilon \rightarrow 0$ ;
- the scheme should be unconditionally stable in the collision step;
- the limiting scheme obtained as  $\varepsilon \rightarrow 0$  is a consistent numerical scheme for the equilibrium subsystem.

**4. Extension of the Nessyahu–Tadmor scheme to the nonhomogeneous case.** Let us consider again the initial value problem (3.1)–(3.2).

We discretize space-time with staggered cells. Following [12], at each time level we reconstruct a piecewise linear approximation of the form

$$L_j(x, t) = u_j(t) + \frac{x - x_j}{\Delta x} u'_j, \quad x_{j-1/2} \leq x \leq x_{j+1/2},$$

where  $u'_j/\Delta x$  is a first order approximation of the space derivative at  $x_j$ . By integrating (3.1) over the cell  $[x_j, x_{j+1}] \times [t^n, t^{n+1}]$ , we obtain

$$(4.1) \quad \begin{aligned} u_{j+1/2}^{n+1} &= \frac{1}{2}(u_j^n + u_{j+1}^n) + \frac{1}{8}(u'_j - u'_{j+1}) + \frac{1}{\Delta x} \int_{t^n}^{t^{n+1}} f(u(x_j, t)) - f(u(x_{j+1}, t)) dt \\ &+ \frac{1}{\Delta x} \int_{t^n}^{t^{n+1}} \int_{x_j}^{x_{j+1}} g(u(x, t)) dx dt. \end{aligned}$$

Different schemes are obtained by suitable discretization of the integrals of fluxes and source.

The integral of the flux is discretized by midpoint rule

$$\int_{t^n}^{t^{n+1}} f(u(x_j, t)) dt \approx \Delta t f(u_j^{n+1/2}).$$

The predictor  $u_j^{n+1/2}$  is obtained from Taylor expansion by an explicit scheme

$$u_j^{n+1/2} = u_j^n + \frac{\Delta t}{2} \left( g(u_j^n) - \frac{f'_j}{\Delta x} \right),$$

or by an implicit scheme

$$u_j^{n+1/2} = u_j^n + \frac{\Delta t}{2} \left( g(u_j^{n+1/2}) - \frac{f'_j}{\Delta x} \right),$$

which is appropriate for stiff problems in order to avoid restriction on the time step.

The values of  $u'_j$  and  $f'_j$  can be explicitly computed as illustrated in section 3.

Several quadrature formulas have been tested for discretizing the integral of the source term. The main guideline to select the appropriate quadrature formula in order to get a uniformly accurate scheme in  $\varepsilon$  is to choose nodes and weights that give an  $L$ -stable scheme for the stiff part (see the next section for the stability analysis).

Here we show several possible choices. Consistency and stability analysis will be used to select schemes suitable also in the fluid limit.

An example of a scheme with explicit corrector is obtained by using a quadrature formula which is midpoint in time and trapezoidal rule in space

$$(4.2) \quad I_g = \int_{t^n}^{t^{n+1}} \int_{x_j}^{x_{j+1}} g(u(x, t)) \, dx dt \approx \frac{1}{2} \left( g(u_j^{n+1/2}) + g(u_{j+1}^{n+1/2}) \right) \Delta x \Delta t.$$

The predictor values  $u_j^{n+1/2}$  may be computed by an explicit or an implicit step. An example of a scheme with implicit corrector is obtained by

$$(4.3) \quad I_g \approx \hat{g}_{j+1/2}^{n+1/2} = \frac{1}{2} \left( \frac{g(u_{j+1}^n) + g(u_j^n)}{2} + g(u_{j+1/2}^{n+1}) \right) \Delta x \Delta t$$

which leads to the implicit central scheme of order 2 (ICS2)

$$(4.4) \quad \begin{aligned} u_{j+1/2}^{n+1} - \frac{\Delta t}{2} g(u_{j+1/2}^{n+1}) &= \frac{1}{2}(u_j^n + u_{j+1}^n) + \frac{1}{8}(u'_j - u'_{j+1}) \\ -\lambda \left( f(u_{j+1}^{n+1/2}) - f(u_j^{n+1/2}) \right) &+ \frac{\Delta t}{4} (g(u_j^n) + g(u_{j+1}^n)). \end{aligned}$$

We observe that in the simple case when  $f \equiv 0$ , the scheme can be regarded as a numerical scheme for systems of ordinary differential equations (ODEs). More precisely, scheme ICS2 becomes the trapezoidal method (or Crank–Nicolson), which is  $A$ -stable, but not  $L$ -stable [33], and therefore it is not suitable for strongly stiff systems, such as the hyperbolic system near the fluid dynamic regime. For an explicit example in this context consult [25].

The choice of a Radau quadrature formula leads to the uniformly implicit central scheme of order 2 (UCS2)

$$(4.5) \quad \begin{aligned} u_{j+1/2}^{n+1} &= \frac{1}{2}(u_j^n + u_{j+1}^n) + \frac{1}{8}(u'_j - u'_{j+1}) - \lambda \left( f(u_{j+1}^{n+1/2}) - f(u_j^{n+1/2}) \right) \\ &+ \Delta t \left( \frac{3}{8}g(u_j^{n+1/3}) + \frac{3}{8}g(u_{j+1}^{n+1/3}) + \frac{1}{4}g(u_{j+1/2}^{n+1}) \right). \end{aligned}$$

In the implicit methods ICS2 and UCS2, the values of  $u_j^{n+1/2}$  and  $u_j^{n+1/3}$  are evaluated with an implicit predictor step,

$$\begin{aligned} u_j^{n+1/2} &= u_j^n + \frac{\Delta t}{2} \left( g(u_j^{n+1/2}) - \frac{f'_j}{\Delta x} \right), \\ u_j^{n+1/3} &= u_j^n + \frac{\Delta t}{3} \left( g(u_j^{n+1/3}) - \frac{f'_j}{\Delta x} \right). \end{aligned}$$

Standard truncation analysis shows that UCS2 is second order accurate in space and time in the rarefied regime (i.e., when  $\varepsilon \ll 1$ ).

Concerning the fluid limit, we observe that when  $f \equiv 0$ , the scheme is an  $L$ -stable scheme for systems of ODEs (see section (5.2)), and therefore the scheme provides the correct limit as  $\varepsilon \rightarrow 0$ . A more detailed analysis of this scheme is presented in the next section.

### 5. Analysis of scheme UCS2.

**5.1. Consistency analysis.** In this section we perform a consistency analysis of scheme UCS2. We shall show that the scheme is second order accurate both in the rarefied regime ( $\varepsilon = 1$ ) and the fluid dynamic limit ( $\varepsilon = 0$ ). We apply the scheme to the simple  $2 \times 2$  system

$$\begin{aligned} (5.1) \quad & u_t + v_x = 0, \\ & v_t + u_x = -\frac{1}{\varepsilon}(v - au), \\ (5.2) \quad & u(x, 0) = u^0(x), \quad v(x, 0) = v^0(x), \end{aligned}$$

where  $a \in \mathbf{R}$ ,  $|a| < 1$ . The accuracy of the scheme is studied by comparing the Taylor expansion in time of the exact solution and of the numerical solution after one time step. In the fluid dynamic limit  $v = au$ , and the system reduces to the single equation

$$\begin{aligned} (5.3) \quad & u_t + au_x = 0, \\ (5.4) \quad & u(x, 0) = u^0(x). \end{aligned}$$

For small value of  $\varepsilon$ , the behavior of the system is described by the Navier–Stokes limit

$$\begin{aligned} (5.5) \quad & u_t + au_x = \varepsilon(1 - a^2)u_{xx}, \\ (5.6) \quad & v = au - \varepsilon(1 - a^2)u_x, \\ (5.7) \quad & u(x, 0) = u^0(x). \end{aligned}$$

We shall consider separately the different regimes.

*Rarefied regime:*  $\varepsilon = 1$ . The Taylor expansion of the exact solution is given by

$$\begin{aligned} (5.8) \quad & u(x, \Delta t) = u^0 - \Delta t v_x^0 + \frac{1}{2} \Delta t^2 (u_{xx}^0 + v_x^0 - au_x^0) + O(\Delta t^3), \\ (5.9) \quad & v(x, \Delta t) = v^0 - \Delta t (u_x^0 + v^0 - au^0) + \frac{1}{2} \Delta t^2 (v_{xx}^0 + u_x^0 - av_x^0 - au^0) + O(\Delta t^3), \end{aligned}$$

with an obvious notation.

*Fluid dynamic limit:*  $\varepsilon = 0$ . The Taylor expansion of the exact solution is given by

$$(5.10) \quad u(x, \Delta t) = u^0 - \Delta t au_x^0 + \frac{1}{2} \Delta t^2 a^2 u_{xx}^0 + O(\Delta t^3).$$

*Thin regime:*  $\varepsilon \ll 1$ . The Taylor expansion of the exact solution is given by

$$(5.11) \quad \begin{aligned} u(x, \Delta t) = & u^0 - \Delta t au_x^0 + \frac{1}{2} \Delta t^2 a^2 u_{xx}^0 + \varepsilon \Delta t (1 - a^2)(u_{xx}^0 - a \Delta t u_{xxx}^0) \\ & + O(\Delta t^3, \varepsilon^2). \end{aligned}$$

The above expressions are valid for the point-wise value of the exact solution. Similar expressions can be derived for the cell average  $\bar{u}(x, t)$  defined as

$$\bar{u}(x, t) = \frac{1}{h} \int_{-h/2}^{h/2} u(x + \xi, t) d\xi.$$

To the same order of accuracy, the expressions for the Taylor expansion of the solution are the same, except that  $u^0(x)$  will be substituted by

$$\bar{u}^0(x) \equiv \frac{1}{h} \int_{-h/2}^{h/2} u^0(x + \xi) d\xi,$$



where  $h \equiv \Delta x$ . The relation between  $u^0(x)$  and  $\bar{u}^0(x)$  for a smooth function is

$$u^0(x) = \bar{u}^0(x) - \frac{1}{24}u_{xx}^0(x)h^2 + O(h^4).$$

By applying scheme UCS2 to system (5.1), one computes  $\bar{u}_{j+1/2}^1$  and  $\bar{v}_{j+1/2}^1$  as regular functions of  $\varepsilon, h, \lambda$

$$(5.12) \quad \bar{u}_{j+1/2}^1 = \mathcal{U}(U_j, U_{j+1}, U'_j, U'_{j+1}, \lambda, h, \varepsilon),$$

$$(5.13) \quad \bar{v}_{j+1/2}^1 = \mathcal{V}(U_j, U_{j+1}, U'_j, U'_{j+1}, \lambda, h, \varepsilon),$$

where for brevity we denote by  $U$  the field variables  $(\bar{u}, \bar{v})$ . Direct computation shows that

$$\mathcal{V}(\cdot, \varepsilon = 0) = a\mathcal{U}(\cdot, \varepsilon = 0).$$

The dependence on  $\varepsilon$  is regular, and the function can be expanded in  $\varepsilon$ . To zeroth order in  $\varepsilon$  one has

$$(5.14) \quad \bar{u}_{j+1/2}^1 = \frac{1}{2}(\bar{u}_j^0 + \bar{u}_{j+1}^0) - \frac{1}{8}(u'_{j+1} - u'_j) - \lambda a(\bar{u}_{j+1}^0 - \bar{u}_j^0) + \frac{1}{2}a\lambda^2(v'_{j+1} - v'_j).$$

The Taylor expansion of the exact solution is given by (5.10), which, for the cell average, becomes

$$(5.15) \quad \bar{u}(x_{j+1/2}, \lambda h) = \bar{u}^0(x_{j+1/2}) - \lambda h a u_x^0(x_{j+1/2}) + \frac{1}{2}\lambda^2 h^2 a^2 u_{xx}^0(x_{j+1/2}) + O(h^3).$$

For a regular initial condition with

$$(5.16) \quad v^0(x) = a u^0(x)$$

one has

$$(5.17) \quad \begin{aligned} \bar{u}^0(x_{j+1/2}) &= \frac{1}{2}(\bar{u}_j^0 + \bar{u}_{j+1}^0) - \frac{1}{8}(u'_{j+1} - u'_j) + O(h^3), \\ u_x^0(x_{j+1/2}) &= \frac{1}{h}(\bar{u}_{j+1}^0 - \bar{u}_j^0) + O(h^2), \\ v_{xx}^0(x_{j+1/2}) &= \frac{1}{h^2}(v'_{j+1} - v'_j) + O(h). \end{aligned}$$

These expressions can be easily proved under the following assumptions:

- (i) the function  $u^0(x)$  is smooth;
- (ii) the approximation of the derivatives is first order accurate but depends smoothly on  $x$ , i.e.,

$$(5.18) \quad \begin{aligned} \frac{u'_j}{h} &= \frac{\partial u^0}{\partial x}(x_j) + c(x_j)h + O(h^2), \\ \frac{v'_j}{h} &= \frac{\partial v^0}{\partial x}(x_j) + d(x_j)h + O(h^2) \end{aligned}$$

with  $c(x)$  and  $d(x)$  smooth.

Making use of relations (5.14), (5.15), (5.17), one obtains

$$\bar{u}_{j+1/2}^1 - \bar{u}(x_{j+1/2}, \lambda h) = O(h^3)$$

and therefore the scheme is second order accurate in the fluid dynamic limit.

*Analysis for  $\varepsilon = 1$ .* In order to check the accuracy for  $\varepsilon = 1$ , we expand the numerical solution  $(\bar{u}_{j+1/2}^1, \bar{v}_{j+1/2}^1)$  making use of the following Taylor expansion around  $x_{j+1/2}$ :

$$\begin{aligned}
 \bar{u}_{j+1} &= \bar{u}_{j+1/2} + \frac{1}{2}u_x h + \frac{1}{8}u_{xx}h^2 + O(h^3), \\
 \bar{u}_j &= \bar{u}_{j+1/2} - \frac{1}{2}u_x h + \frac{1}{8}u_{xx}h^2 + O(h^3), \\
 \frac{u'_{j+1}}{h} &= u_x + \left(c + \frac{1}{2}u_{xx}\right)h + O(h^2), \\
 \frac{u'_j}{h} &= u_x + \left(c - \frac{1}{2}u_{xx}\right)h + O(h^2),
 \end{aligned}
 \tag{5.19}$$

where  $\bar{u} = \bar{u}(x_{j+1/2})$ ,  $u_x \equiv u_x(x_{j+1/2})$ ,  $u_{xx} \equiv u_{xx}(x_{j+1/2})$ ,  $c \equiv c(x_{j+1/2})$ . Analogous formulae hold for  $v$ . These expansions are in agreement with expressions (5.17) and (5.18).

Substituting the expansion into the expression of  $\mathcal{U}$  and  $\mathcal{V}$ , and making use of (5.17), one obtains

$$\begin{aligned}
 \bar{u}_{j+1/2}^1 &= \bar{u}^0 - h\lambda v_x^0 + \frac{1}{2}h^2\lambda^2(v_x^0 - au_x^0 + u_{xx}^0) + O(h^3), \\
 \bar{v}_{j+1/2}^1 &= \bar{v}^0 + \lambda(a\bar{u}^0 - \bar{v}^0 - u_x) + \frac{1}{2}h^2\lambda^2(\bar{v}^0 - a\bar{u}^0 + u_x^0 - av_x^0 + v_{xx}^0) + O(h^3),
 \end{aligned}$$

which is in agreement with the Taylor expansion of the exact solution.

*Analysis for  $\varepsilon \ll 1$ .* The Taylor expansion in  $h$  and  $\varepsilon$  of the numerical solution  $\mathcal{U}$  is

$$\bar{u}_{j+1/2}^1 = \bar{u}^0 - h\lambda au_x^0 + \frac{1}{2}h^2\lambda^2 v_{xx}^0 + \varepsilon h\lambda(u_{xx}^0 - av_{xx}^0) + 2\varepsilon(au_x^0 - v_x^0) + O(\varepsilon^2).$$

Assuming that the initial condition is in agreement with the Chapman–Enskog expansion of the solution of system (5.1), i.e., that

$$v^0 = au^0 + O(\varepsilon),$$

then the term  $2\varepsilon(av_x^0 - v_x^0)$  can be neglected since it is  $O(\varepsilon^2)$ , and the numerical solution is in agreement with the exact solution (5.11), if we neglect terms  $O(h^3, \varepsilon h^2, \varepsilon^2)$ .

**5.2. Stability analysis.** In this section we perform the linear stability analysis of the scheme. We consider the scheme as applied to a system of ODEs and study its  $A$ -stability property.

First let us briefly recall the definition of  $A$ - and  $L$ -stability. Let us consider a system of ODEs of the form

$$y' = f(y),
 \tag{5.20}$$

$$y(0) = y_0,
 \tag{5.21}$$

where  $y \in \mathbf{R}^m$ . In order to study  $A$ -stability of a one-step scheme (e.g., a Runge–Kutta scheme), let us apply the scheme to the test equation

$$y' = \lambda y,
 \tag{5.22}$$

$$y(0) = 1,
 \tag{5.23}$$

with  $y \in \mathbf{C}$  and  $\lambda \in \mathbf{C}$ ,  $\Re\lambda < 0$ . The exact solution of this equation at time  $n\Delta t$  is

$$y(n\Delta t) = \exp(\lambda n\Delta t)$$

and its absolute value decreases monotonically in time. When we apply a one-step method to the test equation, the numerical solution at time  $n\Delta t$  is

$$y_n = (y_1)^n,$$

where  $y_1 = \mathcal{R}(\lambda\Delta t)$  is the numerical solution after one step. The function  $\mathcal{R}(\lambda\Delta t)$  is called *function of absolute stability*. The region of the complex plane

$$S_A = \{z \in \mathbf{C} : |\mathcal{R}(z)| \leq 1\}$$

is called *region of absolute stability*. A one-step scheme is said to be *A-stable* if its region of absolute stability contains the complex half plane  $\mathbf{C}^- = \{z \in \mathbf{C} : \Re z \leq 0\}$ .

A scheme is said to be *L-stable* if it is *A-stable* and  $\lim_{z \rightarrow \infty} \mathcal{R}(z) = 0$ . *L-stability* is important when dealing with stiff systems. For a discussion of different concepts of stability and stiffness for systems of ODEs, see, for example, [33].

Now we generalize the concept of *A-stability* to systems of equations which are the sum of stiff and nonstiff parts. Let us consider a system of the form

$$(5.24) \quad y' = f(y) + g(y),$$

$$(5.25) \quad y(0) = y_0.$$

The time discretization of scheme UCS2 is particularly suited for systems of the form (5.24), where it is possible to identify a stiff part,  $g$ , and a nonstiff part,  $f$ . Sometimes, such as in the case of hyperbolic systems with relaxation, the computation of nonstiff part is expensive, and therefore it would be desirable to do it explicitly.

The scheme that we used can be written in the form

$$(5.26) \quad \begin{aligned} Y_{1/2} &= y_0 + \frac{k}{2}f(y_0) + \frac{k}{2}g(Y_{1/2}), \\ Y_{1/3} &= y_0 + \frac{k}{3}f(y_0) + \frac{k}{3}g(Y_{1/3}), \\ y_1 &= y_0 + kf(Y_{1/2}) + \frac{k}{4}(3g(Y_{1/3}) + g(y_1)), \end{aligned}$$

where  $k$  denotes the time step, and  $y_1$  denotes the numerical solution after one time step.

Standard truncation analysis shows that  $y(k) - y_1 = O(k^3)$ , therefore the scheme is of order 2.

In order to study the stability, we first show that the scheme is *L-stable* when  $f \equiv 0$ . Then we study the restrictions on the time step in the general case.

In order to study the *A-stability*, we consider the model problem

$$(5.27) \quad y' = \lambda_1 y + \lambda_2 y,$$

$$(5.28) \quad y(0) = 1.$$

When applied to this equation, scheme (5.26) gives

$$(5.29) \quad y_1 = \mathcal{R}(z_1, z_2) = \left(4 + 4z_1 \frac{2 + z_1}{2 - z_2} + 3z_2 \frac{3 + z_1}{3 - z_2}\right) (4 - z_2)^{-1},$$

where  $z_1 = \lambda_1 k, z_2 = \lambda_2 k$ . The function  $\mathcal{R}(z_1, z_2)$  is the *function of absolute stability*. In the case  $z_1 = 0$  the function reduces to

$$\mathcal{R}(0, z_2) = \frac{12 + 5z_2}{(3 - z_2)(4 - z_2)}.$$

A simple calculation shows that this corresponds to the stability function of an  $L$ -stable scheme.

The *region of absolute stability*  $S_A$  associated with scheme (5.26) is defined as

$$S_A = \{(z_1, z_2) \in \mathbf{C}^2 : |\mathcal{R}(z_1, z_2)| \leq 1\}.$$

It is evident that the region does not contain the set  $\mathbf{C}^- \times \mathbf{C}^-$ . Our goal is to show that there exist two regions of the complex plane,  $S_1 \subset \mathbf{C}, S_2 \subset \mathbf{C}$ , with the following properties:

$$(5.30) \quad S_A \supset S_1 \times S_2,$$

$$(5.31) \quad S_2 \supset \mathbf{C}^- \equiv \{z \in \mathbf{C} : \Re(z) \leq 0\},$$

and to compute them. It is clear that two such sets, if they exist, are not unique. We shall compute explicitly the largest set  $S_1$  for which  $S_2 \supset \mathbf{C}^-$ . Such a region is defined by

$$S_1 = \left\{ z_1 \in \mathbf{C} : \max_{z_2 \in \mathbf{C}^-} |\mathcal{R}(z_1, z_2)| \leq 1 \right\}.$$

In order to proceed we make use of the following lemma.

LEMMA 5.1. *For any fixed  $z_1 \in \mathbf{C}$ , the function  $|\mathcal{R}(z_1, z_2)|$  assumes its maximum value in  $\mathbf{C}^-$  for some  $z_2$  belonging to the imaginary axis.*

*Proof.* For any fixed value  $z_1$ , the function  $\mathcal{R}(z_1, z_2)$  is analytic in  $z_2$ , olomorphic in  $\mathbf{C}^-$ . Therefore the maximum value of the function in  $\mathbf{C}^-$  is obtained for some value of  $z_2 \in \partial\mathbf{C}^-$ . Furthermore, we observe that

$$\lim_{z_2 \rightarrow \infty} \mathcal{R}(z_1, z_2) = 0;$$

therefore the maximum of  $|\mathcal{R}(z_1, z_2)|$  occurs on the imaginary axis. □

From the above lemma, we can write

$$S_1 = \{z_1 \in \mathbf{C} : \max_{y \in \mathbf{R}} |\mathcal{R}(z_1, iy)| \leq 1\}.$$

The boundary of this region (boundary locus) will be obtained as

$$\partial S_1 = \{z_1 \in \mathbf{C} : \max_{y \in \mathbf{R}} |\mathcal{R}(z_1, iy)| = 1\}.$$

Such a set is not empty. In fact it contains point  $z_1 = 0$ . In order to compute  $S_1$  we proceed as follows. Let us define the function

$$F(\theta, \rho, y) = |\mathcal{R}(-1 + \rho e^{i\theta}, iy)|^2, \quad \theta \in [-\pi, \pi), y \in \mathbf{R}.$$

Direct calculation shows that

$$F(\theta, \rho, y) = \frac{N(\theta, \rho, y)}{D(\theta, \rho, y)},$$

with

$$\begin{aligned}
 N &= (144 + 16y^2)\rho^4 \\
 &+ ((144y + 24y^3)\sin\theta + 24y^2\cos\theta)\rho^3 \\
 &+ ((160y^2 + 576)\cos^2\theta + 32y^3\cos\theta\sin\theta + 9y^4 - 44y^2 - 288)\rho^2 \\
 &+ ((24y^2 + 12y^4)\cos\theta - (144y + 48y^3)\sin\theta)\rho \\
 &+ 64y^2 + 144 + 4y^4, \\
 D &= 576 + 244y^2 + 29y^4 + y^6,
 \end{aligned}$$

and let us define  $F_s(\theta, \rho, y) = N(\theta, \rho, y) - D(\theta, \rho, y)$ . Now let

$$\mathcal{H}(\theta, \rho) = \max_{y \in \mathbf{R}} F_s(\theta, \rho, y).$$

The boundary of  $S_1$  can therefore be expressed in terms of  $\mathcal{H}(\theta, \rho)$ ,

$$\partial S_1 = \{(\theta, \rho) : \mathcal{H}(\theta, \rho) = 0\}.$$

The boundary locus can be efficiently computed by a technique similar to the one used to compute the stability region of Runge–Kutta schemes. First observe that  $\mathcal{H}(\theta, 0) < 0$ , therefore  $-1 \in S_1$ . Now let us denote by  $\hat{y}$  the value of  $y$  for which  $\mathcal{H}(\theta, \rho) = F_s(\theta, \rho, y)$ , i.e.,

$$\hat{y}(\theta, \rho) = \arg \max_{y \in \mathbf{R}} F_s(\theta, \rho, y),$$

and let  $\hat{\rho}$  denote the value of  $\rho$  for which  $F_s(\theta, \rho, \hat{y}(\theta, \rho)) = 0$ . Then the boundary locus satisfies the equations

$$(5.32) \quad F_s(\theta, \rho, y) = 0,$$

$$(5.33) \quad G(\theta, \rho, y) \equiv \frac{\partial F_s}{\partial y}(\theta, \rho, y) = 0.$$

The second equation is a consequence of the fact that  $\hat{y}$  is an extremal, and the function  $F_s(\theta, \rho, y)$  is smooth in  $y$ . By differentiating (5.32) and (5.33) one obtains a set of differential equations that defines the boundary locus,

$$(5.34) \quad \frac{d\rho}{d\theta} = F_1(\theta, \rho, y),$$

$$(5.35) \quad \frac{dy}{d\theta} = F_2(\theta, \rho, y),$$

with

$$(5.36) \quad F_1(\theta, \rho, y) = -\frac{\partial F_s / \partial \theta}{\partial F_s / \partial \rho},$$

$$(5.37) \quad F_2(\theta, \rho, y) = -\frac{(\partial G / \partial \theta) + (\partial G / \partial \rho)F_1}{\partial G / \partial y}.$$

The initial condition for the system is

$$y(0) = 0, \quad \rho(0) = 1.$$

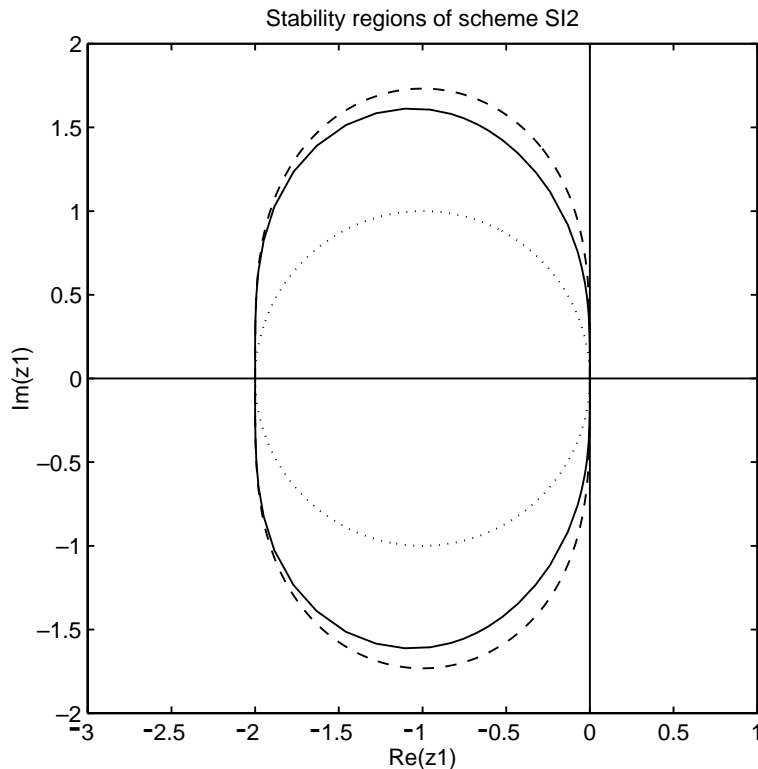


FIG. 1. Stability region in the explicit parameter for scheme UCS2 (continuous line). The dotted and the dashed lines are the stability region of explicit Euler and explicit second order Runge–Kutta, respectively.

The system is solved forward in  $\theta$  in the interval  $[0, \pi]$ , to obtain the upper branch of the boundary locus, and backward, in the interval  $[-\pi, 0]$ , to obtain the lower branch.

The computed stability region is shown in Figure 1. By comparison, the stability region for the explicit Euler scheme and second order Runge–Kutta scheme are shown.

Note that the stability region  $S_1$  contains the stability region of explicit Euler scheme, and it is slightly smaller than the stability of the explicit second order Runge–Kutta.

We remark that the scheme presented here can be effectively used for ODEs where the system can be written in the form (5.24), with  $g$  stiff and  $f$  nonstiff. The scheme is not optimal, since it requires three function evaluations for  $g$  per time step. Improvements and generalizations of the above scheme are under investigation [34].

Similar problems have been considered in [35] and [36]. In the first paper implicit-explicit multistep schemes (IMEX) for the solution of stiff-nonstiff problems have been developed. In the second, several Runge–Kutta schemes have been developed for the same purpose, and their performance is studied in the context of convection-diffusion equations.

The analysis that we performed refers to the generalization of  $A$ -stability analysis common to numerical schemes for systems of ODEs. Note that this result can be used to study the stability for linear systems only if the two matrices that define the system can be diagonalized simultaneously. A more general analysis on linear systems, which

TABLE 1  
*Scheme UCS2: error (in units of  $10^{-3}$ ) for  $\rho$  in the  $L^\infty$  norm.*

Grid points	$\varepsilon = 1$	$\varepsilon = 10^{-1}$	$\varepsilon = 10^{-2}$	$\varepsilon = 10^{-4}$	$\varepsilon = 10^{-6}$	$\varepsilon = 10^{-8}$
100-200	0.17881	0.39626	0.46151	0.45765	0.45786	0.45787
200-400	0.043424	0.096516	0.11976	0.10844	0.10858	0.10859
400-800	0.010726	0.023920	0.034064	0.026575	0.026708	0.026708
800-1600	0.0026675	0.0059636	0.0098711	0.0064981	0.0066124	0.0066126

TABLE 2  
*Scheme UCS2: convergence rate for  $\rho$  in the  $L^\infty$  norm.*

Grid points	$\varepsilon = 1$	$\varepsilon = 10^{-1}$	$\varepsilon = 10^{-2}$	$\varepsilon = 10^{-4}$	$\varepsilon = 10^{-6}$	$\varepsilon = 10^{-8}$
100-200-400	2.04188	2.03761	1.94625	2.07737	2.07609	2.07608
200-400-800	2.01737	2.01253	1.81379	2.02872	2.02349	2.02347
400-800-1600	2.00755	2.00399	1.78697	2.03197	2.01403	2.01401

does not require this assumption will be the subject of future study. A detailed Fourier analysis of the method applied to the test system (5.1) is also under investigation.

**6. Numerical tests.** In this section we perform some numerical tests to assess the accuracy and the shock-capturing properties of the schemes.

*Accuracy tests.* We integrate the equations of the Broadwell model for problems with both smooth and nonsmooth solutions. In all our tests the UNO limiter has been used.

We start our simulations by considering a smooth solution, periodic in space. We integrate system (2.2)–(2.4) with the following initial data:

$$(6.1) \quad \rho(x, 0) = 1 + a_\rho \sin \frac{2\pi x}{L},$$

$$(6.2) \quad u(x, 0) = \frac{1}{2} + a_u \sin \frac{2\pi x}{L},$$

$$(6.3) \quad m(x, 0) = \rho(x, 0)u(x, 0),$$

$$(6.4) \quad z(x, 0) = 0.2z_E(\rho(x, 0)u(x, 0)),$$

where  $z_E$  is the value of  $z$  given by the local Maxwellian, (2.5). Of course the initial value of  $z$  is not Maxwellian.

Several values of  $\varepsilon$  have been considered. The goal of the test is to check uniform convergence of the scheme with respect to  $\varepsilon$ .

The system has been integrated for  $t \in [0, t_f]$ . The values of the parameters used in the computation are

$$L = 20, \quad t_f = 30, \quad a_\rho = 0.3, \quad a_u = 0.1.$$

A mesh with 100, 200, 400, 800, and 1600 grid points has been considered. We call  $\Delta x_1, \Delta x_2, \Delta x_3, \Delta x_4,$  and  $\Delta x_5$  the corresponding values of the mesh size.

The convergence rate is computed from the error according to the formula

$$CR_i = \frac{\log(\text{error}_i/\text{error}_{i+1})}{\log(\Delta x_i/\Delta x_{i+1})},$$

where  $\text{error}_i$  is the error obtained comparing the solutions with  $\Delta x_i$  and  $\Delta x_{i+1}$ .

We shall study only UCS2 because for  $\varepsilon \rightarrow 0$  scheme ICS2 fails to converge unless restrictions on the initial data are imposed. As Tables 1 and 2 show, second order

convergence is obtained in all regimes (with a slight degradation for intermediate regimes).

We remark that the previous results have been obtained in the case that the initial data are not Maxwellian under the CFL condition  $\Delta t/\Delta x = 1/3$  for scheme UCS2 and  $\Delta t/\Delta x = 0.9$  for SPUM.

*Shock capturing tests.* In order to verify the validity of the schemes also on non-smooth solutions, we have considered the Broadwell equations with two different initial data:

RIM1

$$\begin{aligned} \rho = 2, \quad m = 1, \quad z = 1 & \quad \text{for } x < 0.2, \\ \rho = 1, \quad m = 0.13962, \quad z = 1 & \quad \text{for } x > 0.2. \end{aligned}$$

RIM2

$$\begin{aligned} \rho = 1, \quad m = 0, \quad z = 1 & \quad \text{for } x < 0.5, \\ \rho = 0.2, \quad m = 0, \quad z = 1 & \quad \text{for } x > 0.5. \end{aligned}$$

For comparison we integrate the same problem by using also the method proposed in [11], which is a second order splitting scheme with the convection step given by a MUSCL upwind method (hereafter SPUM). The results are reported in Figure 2.

**7. Applications to extended thermodynamics.** In this last section we present a further application of the schemes to the numerical integration of the evolution equations for monatomic gas described in extended thermodynamics. The example is relevant since in this case the analytical expression of the eigenvalues and eigenvectors is not known, and therefore it is preferable to use a numerical scheme that does not require the knowledge of the characteristic structure of the system. Furthermore, the system contains a small parameter that indicates the departure of the system from standard gas dynamics. We study the behavior of the numerical schemes presented in the paper for different values of the relaxation parameter.

Our test consists in the Riemann problem for system (2.6)–(2.11) similar to one proposed by Sod [37], which consists of initial data

RIM3

$$\begin{aligned} \rho = 1, \quad u = 0, \quad p = \frac{5}{3}, \quad \sigma = 0, \quad q = 0 & \quad \text{for } x < 0.5, \\ \rho = \frac{1}{8}, \quad u = 0, \quad p = \frac{1}{6}, \quad \sigma = 0, \quad q = 0 & \quad \text{for } x > 0.5. \end{aligned}$$

Note that these initial conditions coincide with those of the classical Sod problem in terms of conserved quantities, but the gas is different, since here we consider a monatomic gas. The numerical results, therefore, are necessarily different from the classical ones.

For comparison we solve the equations also by the splitting scheme (SPLIT) presented in [25] beside the scheme UCS2. A fixed mesh ratio  $\Delta t = \Delta x/9$  has been used, which is close to the stability limit. For practical applications it is advisable to compute an estimate of the maximum eigenvalue so that an optimal Courant number can be used throughout the calculation.



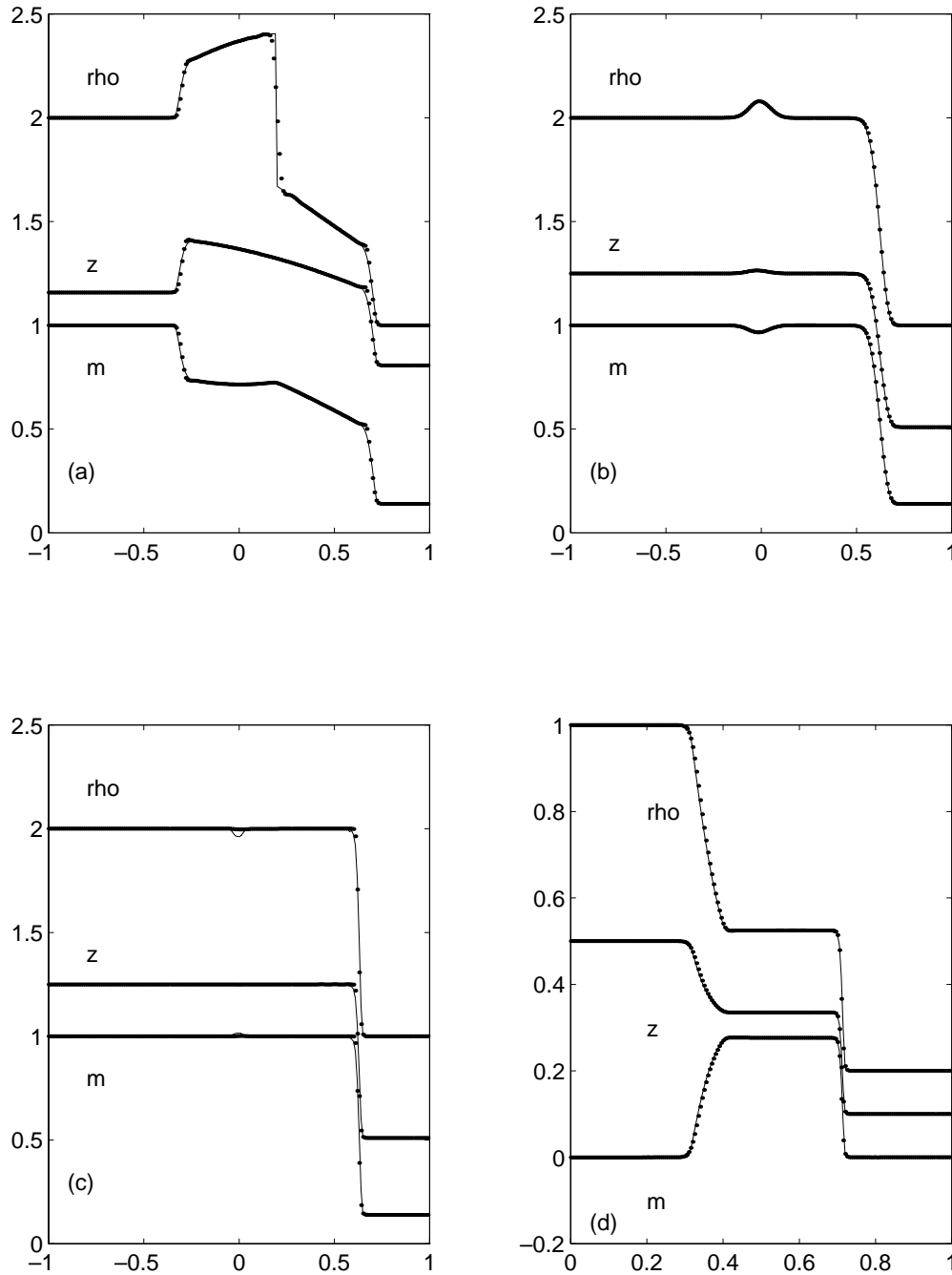


FIG. 2. Comparison of the numerical solutions obtained with UCS2 (dots) and SPUM (continuous line) for the problem RIM1 for the Broadwell model with  $\epsilon = 1$  (case a), with  $\epsilon = 2 \times 10^{-2}$  (case b) and with  $\epsilon = 10^{-8}$  (case c). We used 200 grid points with CFL condition  $\Delta t = \Delta x/3$  for UCS2 while the CFL condition for SPUM is  $\Delta t = 0.9\Delta x$ . The final time is 0.5. (d) shows the solution for initial condition RIM2, with  $\epsilon = 10^{-8}$  and final time 0.25.

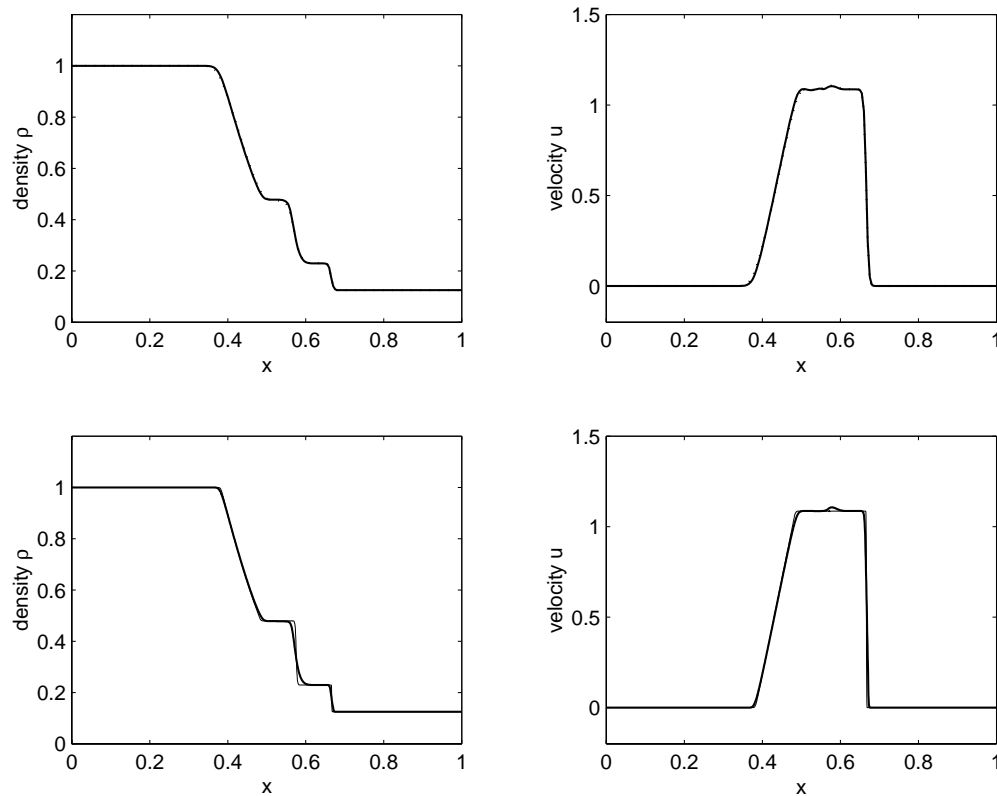


FIG. 3. Solutions at time  $t = 0.07$  of the extended thermodynamics model with  $\varepsilon = 10^{-4}$  for RIM3 initial data and comparison with the solution of the Euler equations of gas dynamics. Mesh ratio  $\Delta t = \Delta x/9$ . Top pictures: density (left) and velocity (right) computed with 200 grid points with UCS2 (continuous line) and SPLIT (dashed line). The thin line represents the reference solution obtained by UCS2 with 1600 grid points. Bottom pictures: density (left) and velocity (right) computed with 1600 grid points. The thin line represents the solution obtained by solving the Euler equations of gas dynamics with the Nessyahu–Tadmor scheme for the same initial value problem (RIM3).

We solve the equations in the  $x$  interval  $[0,1]$ , with  $\varepsilon = 10^{-4}$ , for the same initial value problem. The numerical results at time  $t = 0.07$  are presented in Figures 3 and 4. Figure 3 shows the behavior of the numerical solutions obtained by SPLIT and UCS2 in the calculation of density and velocity, using 200 grid points. The flow appears fully resolved, and very small difference is observed with the solution obtained with 1600 grid points. By comparison, the solution of the same Riemann problem RIM3 for standard gas dynamics is also reported. It appears that the splitting and the nonsplitting scheme give both an accurate description of density and velocity. However, a big difference between the two schemes is observed when computing shear stress and heat flux. The results are presented in Figure 4. It is evident that for these variables scheme UCS2 is much more accurate.

We conclude the paper by remarking that new problems ask for new solutions, and inspire the development of new methods, which often require competences in different fields. This is the case, for example, of recently introduced IMEX schemes [35, 36], where the need for effective tools to solve convection-diffusion problems and the complementary competences in numerical methods for systems of ODEs and PDEs lead to the development of a new class of schemes.

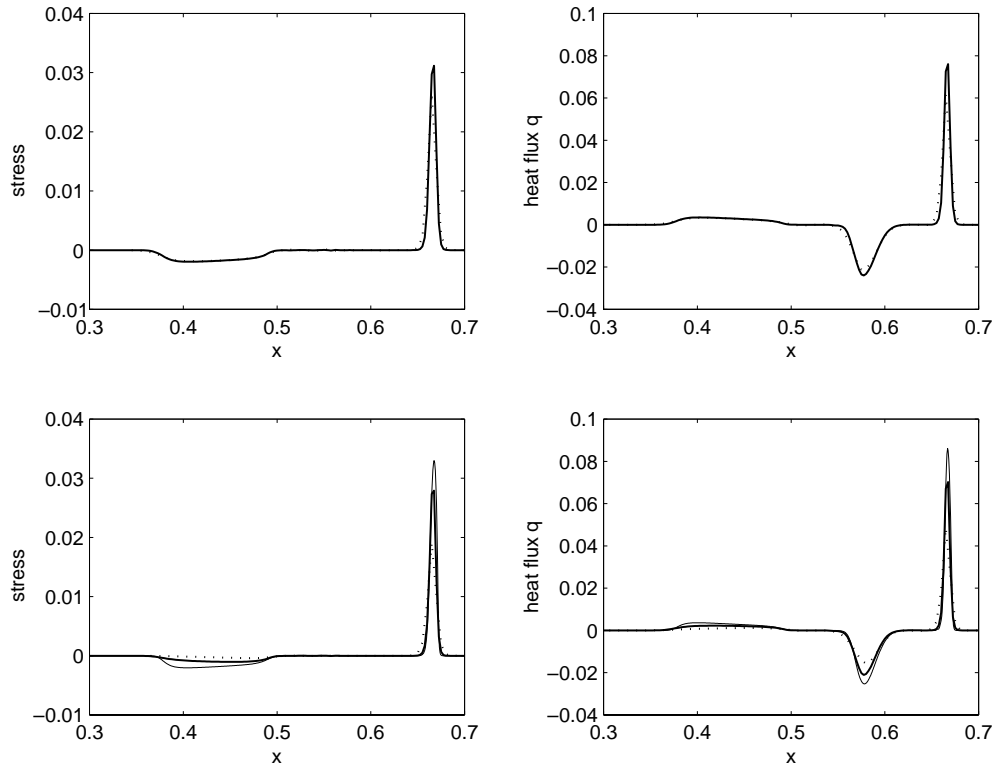


FIG. 4. Solutions of extended thermodynamics model with  $\varepsilon = 10^{-4}$  for RIM3 initial data. Note that the  $x$ -scale has been magnified. Mesh ratio  $\Delta t = \Delta x/9$ . Shear stress (left) and heat flux (right). Top pictures: UCS2 scheme with 200 (dashed line) and 400 (continuous line). Bottom pictures: SPLIT scheme with 200 (dashed line) and 400 (continuous line). The thin line in the bottom pictures is the reference solution obtained by UCS2 with 1600 grid points.

## REFERENCES

- [1] R. GATIGNOL, *Théorie cinétique des gaz à répartition discrète de vitesses*, Lectures Notes in Phys. 36, Springer-Verlag, Berlin, New York, 1975.
- [2] W. VINCENTI AND C. KRUGER, *Introduction to Physical Gas Dynamics*, Krieger Publishing Company, Malabar, FL, 1982.
- [3] A. M. ANILE AND S. PENNISI, *Thermodynamic derivation of the hydrodynamical model for charge transport in semiconductors*, Phys. Rev. B, 46 (1992), pp. 13186–13193.
- [4] A. M. ANILE AND O. MUSCATO, *Improved hydrodynamical model for carrier transport in semiconductors*, Phys. Rev. B, 51 (1995), pp. 16728–16740.
- [5] D. MIHALAS AND B. W. MIHALAS, *Foundations of Radiation Hydrodynamics*, Oxford University Press, New York, 1984.
- [6] E. GODLEWSKI AND P.-A. RAVIART, *Numerical Approximation of Hyperbolic Systems of Conservation Laws*, Springer, New York, 1996.
- [7] R. J. LEVEQUE, *Numerical Methods for Conservation Laws*, 2nd ed., Lectures Math. ETH Zürich, Birkhäuser, Basel, 1992.
- [8] E. TADMOR, *Approximate Solutions of Nonlinear Hyperbolic Equations*, Lecture Notes in Math. 1697, A. Quarteroni, ed., Springer, Berlin, 1998.
- [9] R. B. PEMBER, *Numerical methods for hyperbolic conservation laws with stiff relaxation I. Spurious solutions*, SIAM J. Appl. Math., 53 (1993), pp. 1293–1330.
- [10] S. JIN, *Runge-Kutta methods for hyperbolic systems with stiff relaxation terms*, J. Comp. Phys., 122 (1995), pp. 51–67.
- [11] R. E. CAFLISCH, S. JIN, AND G. RUSSO, *Uniformly accurate schemes for hyperbolic systems with relaxation*, SIAM J. Numer. Anal., 34 (1997), pp. 246–281.

- [12] H. NESSYAHU AND E. TADMOR, *Non-oscillatory central differencing for hyperbolic conservation laws*, J. Comput. Phys., 87 (1990), pp. 408–463.
- [13] R. SANDERS AND W. WEISER, *A high resolution staggered mesh approach for nonlinear hyperbolic systems of conservation laws*, J. Comput. Phys., 101 (1992), pp. 314–329.
- [14] P. ARMINJON, D. STANESCU, AND M. C. VIALON, *A two-dimensional finite volume extension of the Lax-Friedrichs and Nessyahu-Tadmor schemes for compressible flow*, in Proceedings of the 6th International Symposium on Computational Fluid Dynamics, Lake Tahoe, 1995, M. Hafez and K. Oshima, eds., pp. 7–14.
- [15] G.-S. JIANG AND E. TADMOR, *Nonoscillatory central schemes for multidimensional hyperbolic conservation laws*, SIAM J. Sci. Comput., 19 (1998), pp. 1892–1917.
- [16] X.-D. LIU AND E. TADMOR, *Third order nonoscillatory central scheme for hyperbolic conservation Laws*, Numer. Math., 79 (1998), pp. 397–425.
- [17] F. BIANCO, G. PUPPO, AND G. RUSSO, *High order central schemes for hyperbolic systems of conservation laws*, SIAM J. Sci. Comput., 21 (1999), pp. 294–322.
- [18] D. LEVY, G. PUPPO, AND G. RUSSO, *Central WENO schemes for hyperbolic systems of conservation laws*, M2AN Math. Model. Numer. Anal., 33 (1999), pp. 547–571.
- [19] D. LEVY, G. PUPPO, AND G. RUSSO, *A third order central WENO scheme for 2D conservation laws*, Appl. Numer. Math., 33 (2000), pp. 415–421.
- [20] D. LEVY, G. PUPPO, AND G. RUSSO, *Compact central WENO schemes for multidimensional conservation laws*, SIAM J. Sci. Comput., 22 (2000), pp. 656–672.
- [21] A. KURGANOV AND E. TADMOR, *New high-resolution central schemes for nonlinear conservation laws and convection-diffusion equations*, J. Comput. Phys., 160 (2000), pp. 241–282.
- [22] XU-DONG LIU AND S. OSHER, *Convex ENO high order multi-dimensional schemes without field by field decomposition or staggered grids*, J. Comput. Phys., 142 (1998), pp. 304–330.
- [23] G. ERBES, *A High-Resolution Lax-Friedrichs Scheme for Hyperbolic Conservation Laws with Source Terms. Application to the Shallow Water Equations*, Technical Report 62, Department of Meteorology, University of Stockholm, 1993.
- [24] F. BEREUX AND L. SAINSAULIEU, *A higher order method for the solution of hyperbolic systems with relaxation*, Numer. Math., 77 (1997), pp. 143–185.
- [25] S. F. LIOTTA, V. ROMANO, AND G. RUSSO, *Central Schemes for Systems of Balance Laws*, Internat. Ser. Numer. Math. 130, Birkhäuser, Basel, 1999, pp. 651–660.
- [26] E. GABETTA, L. PARESCHI, AND M. RONCONI, *Central schemes for hydrodynamical limits of discrete-velocity kinetic equations*, Transport. Theory Statist. Phys., to appear.
- [27] G. B. WHITHAM, *Linear and Nonlinear Waves*, Wiley, New York, 1974.
- [28] T. P. LIU, *Hyperbolic conservation laws with relaxation*, Comm. Math. Phys., 108 (1987), pp. 153–175.
- [29] I. MÜLLER AND T. RUGGERI, *Rational Extended Thermodynamics*, Springer-Verlag, Berlin, 1998.
- [30] D. JOU, J. CASAS-VAZQUEZ, AND G. LEBON, *Extended Irreversible Thermodynamics*, Springer-Verlag, Berlin, 1993.
- [31] A. HARTEN AND S. OSHER, *Uniformly high-order accurate nonoscillatory schemes. I*, SIAM J. Numer. Anal., 24 (1987), pp. 279–309.
- [32] S. JIN AND C. D. LEVERMORE, *Numerical Schemes for hyperbolic conservation laws with stiff relaxation terms*, J. Comput. Phys., 126 (1996), pp. 449–467.
- [33] E. HAIRER AND G. WANNER, *Solving Ordinary Differential Equations. II. Stiff and Differential-Algebraic Problems*, 2nd ed., Springer Ser. Comput. Math. 14, Springer-Verlag, Berlin, 1996.
- [34] J. BUTCHER, N. GUGLIELMI, AND G. RUSSO, in preparation.
- [35] U. M. ASHER, S. J. RUUTH, AND B. T. R. WETTON, *Implicit-explicit methods for time-dependent partial differential equations*, SIAM J. Numer. Anal., 32 (1995), pp. 797–823.
- [36] U. ASHER, S. RUUTH, AND R. J. SPITERI, *Implicit-explicit Runge-Kutta methods for time dependent partial differential equations*, Appl. Numer. Math., 25 (1997), pp. 151–167.
- [37] G. A. SOD, *A survey of several finite difference methods for systems of nonlinear hyperbolic conservation laws*, J. Comp. Phys., 27 (1978), pp. 1–31.